non peer-reviewed preprint

Functional relationships reveal differences in the water cycle representation of global water models

Sebastian J. Gnann[a,*], Robert Reinecke[a], Lina Stein[a], Yoshihide Wada[b,c], Wim Thiery[d], Hannes Müller Schmied[e,f], Yusuke Satoh[g], Yadu Pokhrel[h], Sebastian Ostberg[i], Aristeidis Koutroulis[j], Naota Hanasaki[k], Manolis Grillakis[j], Simon N. Gosling[l], Peter Burek[c], Marc F. P. Bierkens[m,n], and Thorsten Wagener[a]

[a]Institute of Environmental Science and Geography, University of Potsdam, Potsdam, Germany

[b]Climate and Livability, Biological and Environmental Science and Engineering Division, King Abdullah University of Science and Technology, Thuwal, Saudi Arabia

[c]International Institute for Applied Systems Analysis, Laxenburg, Austria

[d]Department of Hydrology and Hydraulic Engineering, Vrije Universiteit Brussel, Brussels, Belgium

[e]Institute of Physical Geography, Goethe University Frankfurt, Frankfurt am Main, Germany

[f]Senckenberg Leibniz Biodiversity and Climate Research Centre (SBiK-F), Frankfurt am Main, Germany

[g]Moon Soul Graduate School of Future Strategy, Korea Advanced Institute of Science and Technology, Korea

[h]Department of Civil and Environmental Engineering, Michigan State University, East Lansing, MI, USA

[i]Potsdam Institute for Climate Impact Research (PIK), Member of the Leibniz Association, Potsdam, Germany

[j]School of Chemical and Environmental Engineering, Technical University of Crete, Greece

[k]National Institute for Environmental Studies, Tsukuba, Japan

[l]School of Geography, University of Nottingham, Nottingham, United Kingdom

[m]Department of Physical Geography, Utrecht University, The Netherlands

[n]Unit Soil and Groundwater Systems, Deltares, Utrecht, The Netherlands

*Correspondence: gnann1@uni-potsdam.de

Functional relationships reveal differences in the water cycle representation of global water models

Sebastian J. Gnann[a,1,2], **Robert Reinecke**[a,1], **Lina Stein**[a], **Yoshihide Wada**[b,c], **Wim Thiery**[d], **Hannes Müller Schmied**[e,f], **Yusuke Satoh**[g], **Yadu Pokhrel**[h], **Sebastian Ostberg**[i], **Aristeidis Koutroulis**[j], **Naota Hanasaki**[k], **Manolis Grillakis**[j], **Simon N. Gosling**[l], **Peter Burek**[c], **Marc F. P. Bierkens**[m,n], **and Thorsten Wagener**[a]

[a]Institute of Environmental Science and Geography, University of Potsdam, Potsdam, Germany
[b]Climate and Livability, Biological and Environmental Science and Engineering Division, King Abdullah University of Science and Technology, Thuwal, Saudi Arabia
[c]International Institute for Applied Systems Analysis, Laxenburg, Austria
[d]Department of Hydrology and Hydraulic Engineering, Vrije Universiteit Brussel, Brussels, Belgium
[e]Institute of Physical Geography, Goethe University Frankfurt, Frankfurt am Main, Germany
[f]Senckenberg Leibniz Biodiversity and Climate Research Centre (SBiK-F), Frankfurt am Main, Germany
[g]Moon Soul Graduate School of Future Strategy, Korea Advanced Institute of Science and Technology, Korea
[h]Department of Civil and Environmental Engineering, Michigan State University, East Lansing, MI, USA
[i]Potsdam Institute for Climate Impact Research (PIK), Member of the Leibniz Association, Potsdam, Germany
[j]School of Chemical and Environmental Engineering, Technical University of Crete, Greece
[k]National Institute for Environmental Studies, Tsukuba, Japan
[l]School of Geography, University of Nottingham, Nottingham, United Kingdom
[m]Department of Physical Geography, Utrecht University, The Netherlands
[n]Unit Soil and Groundwater Systems, Deltares, Utrecht, The Netherlands
[1]These authors contributed equally to this work.
[2]To whom correspondence should be addressed. E-mail: gnann1@uni-potsdam.de

ABSTRACT

Global water models are increasingly used to understand the past, present, and future water cycle, but disagreements between models make model-based inferences uncertain. While there is empirical evidence of a number of large-scale hydrologic relationships, these relationships are rarely used for model evaluation. Here we evaluate global water models using functional relationships that capture the spatial co-variability of forcing (precipitation, net radiation) and response variables (actual evapotranspiration, groundwater recharge, total runoff). We find strong disagreement in the shape and strength of model-based forcing-response relationships, especially for groundwater recharge. Empirical and theory-derived functional relationships show varying agreements with models, indicating that our process understanding is particularly uncertain for energy balance processes, groundwater recharge processes, and in dry and/or cold regions. Functional relationships offer the potential for fundamental advances in global hydrology and should be a revived focus of hydrological research, with great potential for model evaluation.

1 Main

Global water models – including hydrological, land surface, and dynamic vegetation models[1] – have become increasingly relevant for policy-making and in scientific studies. The Sixth Assessment Report (AR6)[2] of the Intergovernmental Panel on Climate Change (IPCC) draws heavily on results from global water models, which provide information on climate change impacts on hydrological variables including soil moisture[3], streamflow[4,5], terrestrial water storage[6], and groundwater recharge[7]. Some of these models are embedded in global water information services to provide information to a wide array of stakeholders, such as the Global Groundwater Information System[8] or the African Flood and Drought Monitor[9]. Since measurements of many hydrological variables are very sparse and insufficient for large-scale analyses, global water models are also regularly used in scientific studies to provide globally coherent estimates of variables like groundwater recharge and groundwater storage change[10–12].

The IPCC's AR6[2] concludes from an analysis of currently available global water model projections that "uncertainty in future water availability contributes to the policy challenges for adaptation, for example, for managing risks of water scarcity". While some of this uncertainty stems from projected and observed climatic forcing, considerable uncertainty stems from global water models[4,7,13–16]. For instance, Beck et al.[15] found distinct inter-model performance differences when comparing simulated and observed streamflow for 10 global water models driven by the same forcing. To illustrate this uncertainty, we show how 30-year (climatological) averages of actual evapotranspiration, groundwater recharge, and total runoff vary globally, based on outputs from 8 models driven by the same forcing (Figure 1a-c). We find substantial disagreement between models, as indicated by high coefficients of variation, particularly for groundwater recharge and total runoff. We further show which model deviates most from the ensemble mean and find that there is not one model that consistently deviates the most (Figure 1d-f). While this analysis cannot tell us which models perform better or worse, it suggests that it is not straightforward to single out a model for a certain flux or a certain region, which warrants a more in-depth evaluation.

Most evaluation strategies compare model outputs to historical observations over the area for which the observation is representative. This can be at the plot (e.g. flux towers), the catchment (e.g. gauging stations), or grid cell (e.g. gridded remote sensing products) scale. Such approaches are necessary but not sufficient to robustly evaluate global models[17]. First, these approaches compare simulated and observed values location by location, and are therefore limited to improving the model for that location; however, since large fractions of the land area are ungauged, we require methods that can extract and transfer information from gauged to ungauged locations[18]. Second, relevant information for model evaluation might not just lie in comparing the magnitudes of simulated and observed values in a single location, but rather in how a variable varies along a spatial gradient[19]. And third, a comparison with historical observations does not guarantee that a model reliably predicts system behavior under changing conditions[20,21]. Rather than evaluating global models in essentially the same way as catchment-scale models, evidence of a number of large-scale hydrological relationships presents us with an opportunity for a different evaluation strategy that is inherently large-scale, but so far rarely exploited.

Towards a theory of evaluation centered on hydrological relationships

Reviewing the hydrological literature reveals a range of regularities in hydrological relationships[23] that, if they appear in empirical data, should also appear in models (and vice versa). Such relationships often capture behavior that is not prescribed by small-scale processes, but rather emerges through the interaction of these processes (or model components) at large scales. The perhaps most prominent example is the Budyko hypothesis[24], which describes the long-term partitioning of precipitation into evapotranspiration and streamflow solely as a function of the aridity index. Another example are so-called elasticities of streamflow to changing climatic drivers (e.g. precipitation, temperature), which provide an observation-based constraint on climate change impacts on streamflow[25–27]. A third, more recent example are empirical relationships between annual rainfall and runoff, which can be affected differently by prolonged drought; in Australia, some catchments have shown similar rainfall-runoff relationships before and after the Millennium drought, while other catchments have transitioned to a new stable state[28]. The search for robust hydrological relationships is in itself a great scientific challenge[23], but such relationships also provide an excellent yet poorly explored opportunity for model evaluation[29–31].

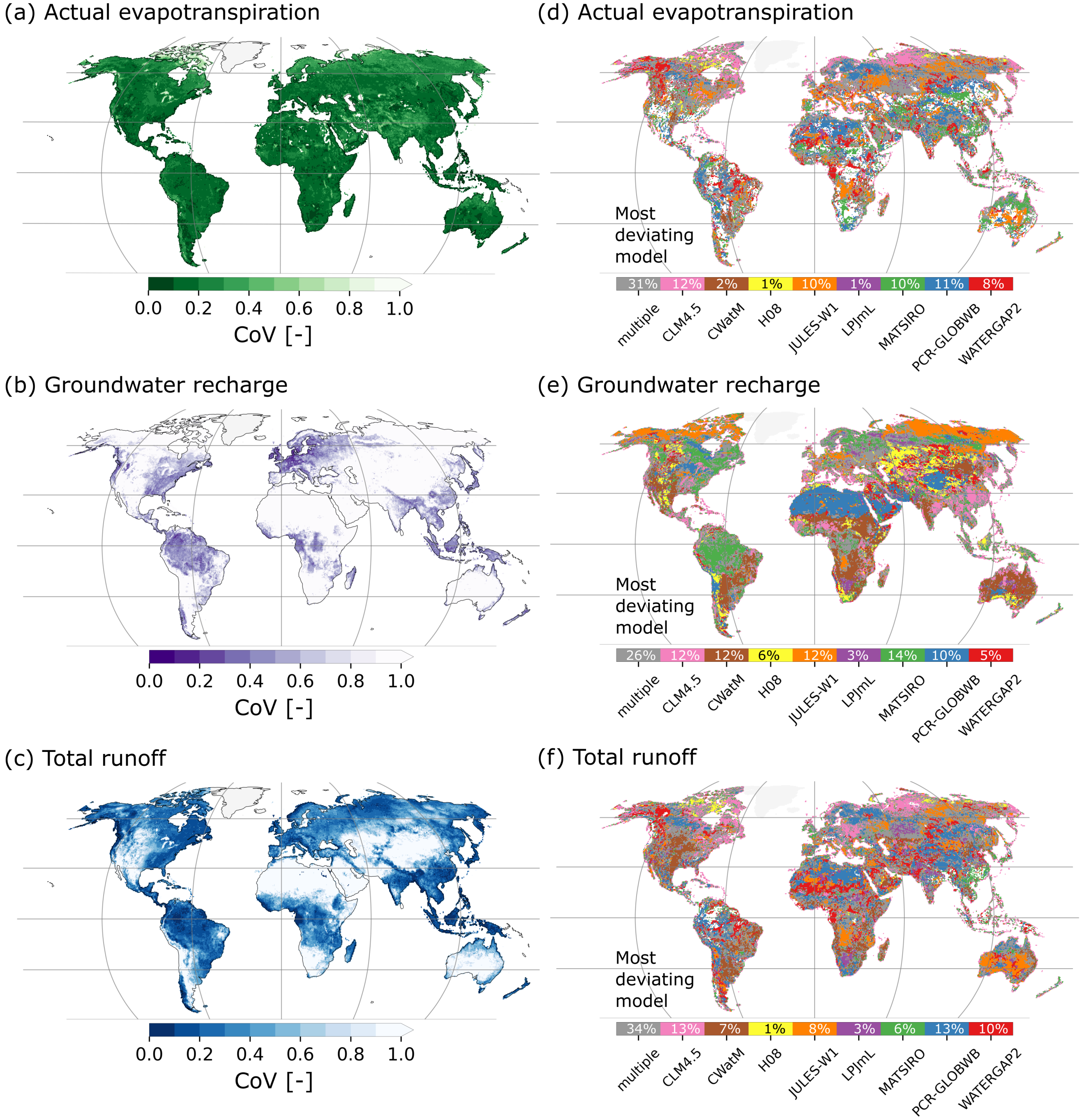

Figure 1. Left: maps showing the coefficient of variation, calculated per grid cell as the standard deviation divided by the mean of 8 global water models for different water fluxes: actual evapotranspiration (a), groundwater recharge (b), and total runoff (c). Lighter areas ("blank spaces"[22]) indicate high CoV values and thus show where models disagree most. Right: maps showing which model deviates most from the ensemble mean for each grid cell for different water fluxes: actual evapotranspiration (d), groundwater recharge (e), and total runoff (f). Dark gray areas in (d)-(f) indicate that multiple models deviate similarly strongly from the ensemble mean. Empty, blank areas in (d)-(f) indicate that no model deviates strongly from the ensemble mean. The percentages shown in (d)-(f) refer to the fraction of grid cells (not land area) covered by each model. Greenland is masked out for the analysis.

Here we focus on functional relationships that capture the spatial co-variability of forcing and response variables[32], well suited to global models due to their gridded nature. While functional relationships have been used before, for example to analyze land surface model functioning[29–31,33], to derive constraints for model regionalization[34], or to calibrate large-scale hydrological models[35,36], their use is scattered among the literature and has not yet been formalized into an evaluation framework. We need to develop a theory of evaluation[37] that does justice to the nature of global models, the purposes for which they are used, and their growing relevance for society[38]. Functional relationships should be central to such a theory of evaluation as they offer several advantages. First, functional relationships can capture how hydrological variables co-vary across large scales, and thus offer the potential for model improvement over large areas. Second, rather than focusing on a process-by-process comparison that can quickly become unmanageable[29], functional relationships capture emergent behavior and explore dominant controls in a top-down manner. And third, functional relationships could also be discovered "in reverse" by first looking for them in models, which would provide hypotheses to be tested and identify the data needed to test them[39]. In what follows, we show how evaluation using functional relationships can help shed new light on model behavior and outline next steps needed to fully realize the potential of this strategy.

We investigate how several forcing and response variables co-vary spatially, both in models and in observational datasets: precipitation P (the available water; equal for all models), net radiation N (a proxy for the available energy), actual evapotranspiration E_a, groundwater recharge R, and total runoff Q (three key water fluxes), all converted to mm/yr. We analyze 30-year (climatological) averages (1975-2004) from 8 global water models (CLM4.5[40], CWatM[41], H08[42], JULES-W1[43], LPJmL[44], MATSIRO[45], PCR-GLOBWB[46], and WaterGAP2[47]) from phase 2b of the Inter-Sectoral Impact Model Intercomparison Project (ISIMIP 2b[48]). We further calculate functional relationships based on several observational datasets and the semi-empirical equation introduced by Budyko[24], listed in Table 1. To explore regional variability in functional relationships[32], we divide the world into four climatic regions: wet-warm (18% of modeled area), wet-cold (15%), dry-cold (24%), and dry-warm (43%), shown in Figure 2d.

2 Results

Strong disagreement in forcing-response relationships between global water models

We can visually assess relationships between forcing (P,N) and response variables (E_a,R,Q) by inspecting scatter plots where each point represents one grid cell (or observation); this is shown for precipitation and groundwater recharge in Figure 2a. We first take a closer look at the shapes of the functional relationships, indicated by the colored lines in Figure 2a. Later we will also quantify the strength of the relationships using Spearman rank correlations ρ_s. We stick to a qualitative discussion, given that fitting an equation would mean that we would have to assume a functional form. We report mean values and slopes (obtained via linear regression) for each region in the Supplementary Information (Tables S4-S7), which quantitatively support our visual assessment here, but are not shown for brevity. Figure 3 shows connected binned median values for precipitation and the three water fluxes for all models and observational datasets (see Table 1), separated by climate region.

While the P-E_a-relationships look similar in shape, they can differ greatly in magnitude (Figure 3). They increase rather linearly in dry (water-limited) regions, and first increase and then flatten out in wet (energy-limited) regions. This flattening is related to reaching an energy limit that bounds actual evapotranspiration despite increasing precipitation. The limit differs greatly between models, up to about 400 mm/yr in wet-warm places. Since all models are forced with the same total radiation, this difference must be related to the way the models translate total radiation into net radiation, and how they then use net radiation to calculate actual evapotranspiration (note that there is no obvious connection to the different potential evapotranspiration schemes used[49]). In dry regions, actual evapotranspiration is mostly limited by precipitation, which is the same for all models, resulting in less variability. The Budyko equation and FLUXCOM[50] data suggest, in line with literature estimates[51], that most models underestimate actual evapotranspiration, often greatly so (see Tables S4 and S5 in the Supplementary Information).

Most P-R-relationships increase monotonically, but the shape, the slope, and the threshold after which some models start to produce groundwater recharge are very different (Figure 3). For instance, in dry-warm regions, some models produce essentially no groundwater recharge even if precipitation is above 1000 mm/yr, while others

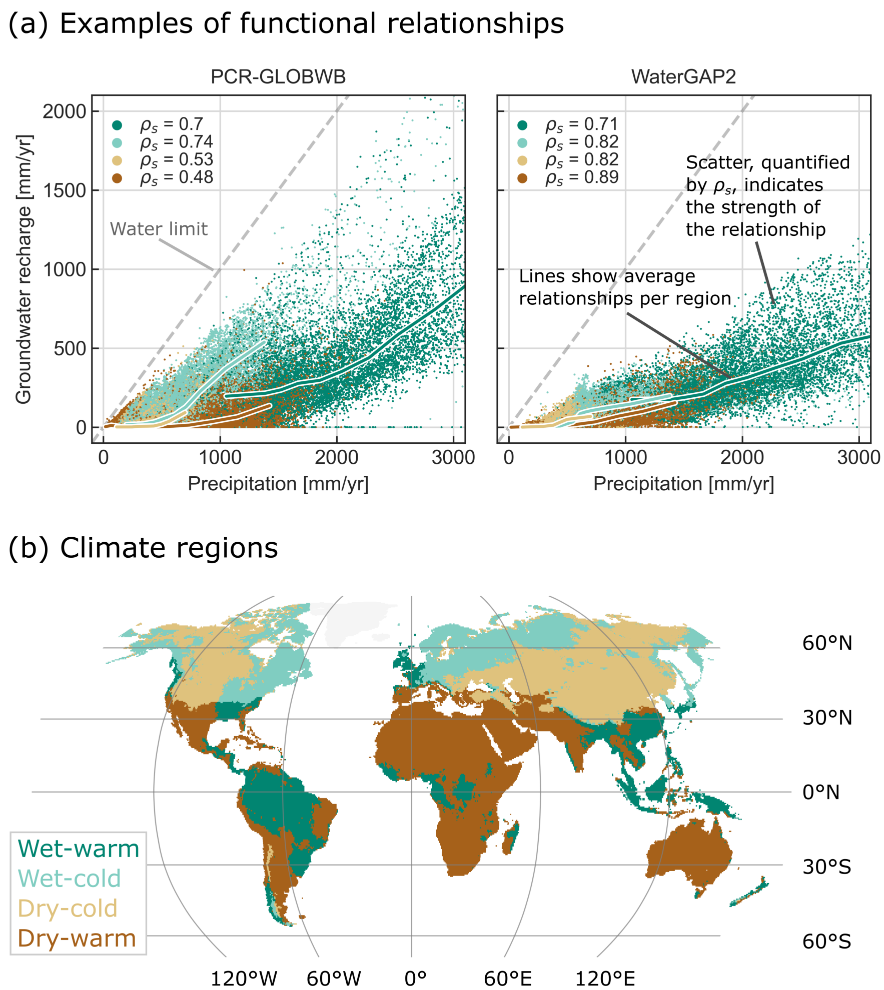

Figure 2. (a) Scatter plots between precipitation and groundwater recharge for PCR-GLOBWB and WaterGAP2. Due to space constraints, we focus on a few examples with differing relationships. Scatter plots for all variable pairs are shown in Figures S15-20 in the Supplementary Information. Each dot represents one grid cell and is based on the 30-year average of each flux. Spearman rank correlations ρ_s measure the strength of the relationship between forcing and response variables and are calculated for all grid cells within a climate region. The lines connect binned medians (10 bins along the x-axis with equal amount of points per bin) for each region. The climate regions are shown in (b). The dashed line shows the 1:1 line, indicating the water limit assuming all water is supplied by precipitation.

produce over 200 mm/yr. In dry-warm regions we have by far the best database on groundwater recharge[52,53], and the observations fall (apart from very high precipitation values) within the range of the models. In wet-warm regions we find the largest disagreement between models and observations, which suggest lower (higher) groundwater recharge rates for higher (lower) precipitation. While this shows the benefit of using an ensemble rather than a single model, even a large ensemble spread does not always capture the observed relationships. The large spread further suggests that many models greatly over- or underestimate groundwater recharge rates, and consequently greatly over- or underestimate how much groundwater contributes to evapotranspiration and streamflow[54]. The differences in slope, visible for all climate regions, reflect very different spatial sensitivities to changes in precipitation. Whether temporal sensitivities are similar can only be hypothesized given that no global dataset with groundwater recharge time series is available, but would imply very different responses to projected changes in precipitation.

The P-Q-relationships look similar in shape and mostly increase monotonically, especially for wet regions

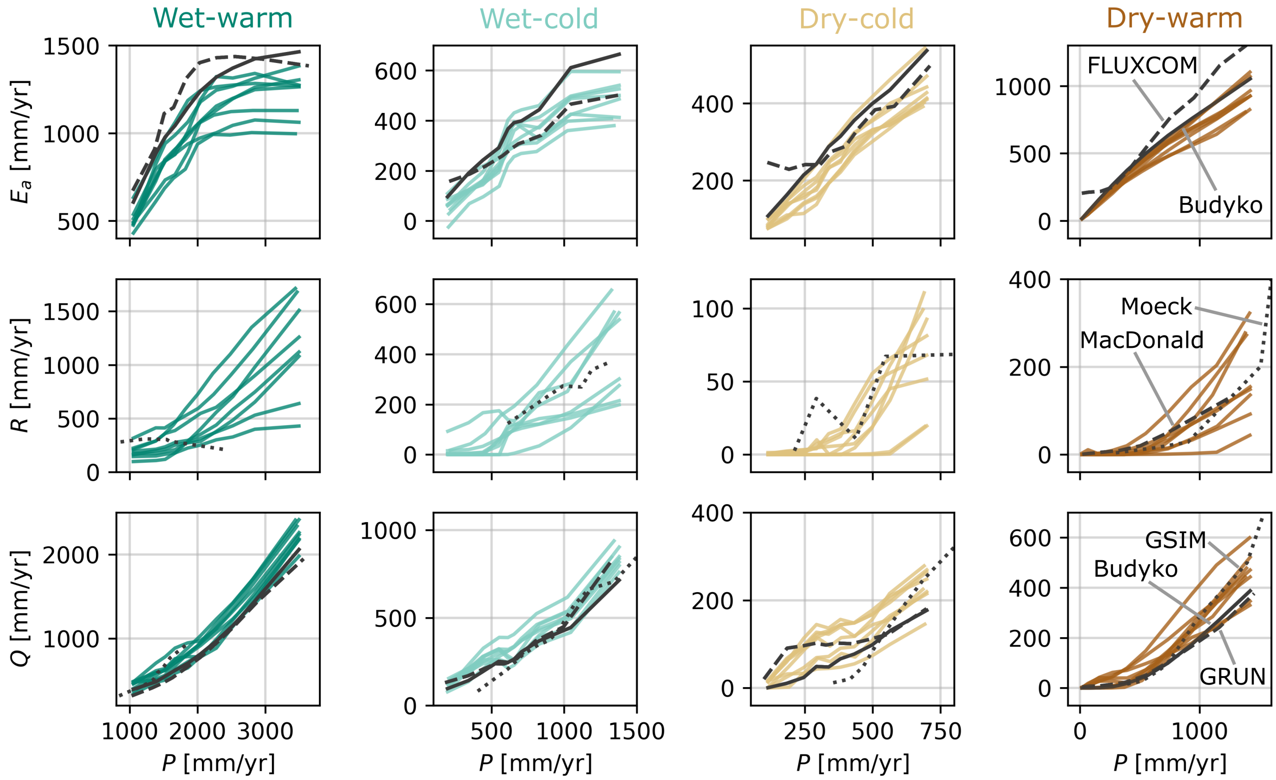

Figure 3. Average model-based and observation-based functional relationships between precipitation P and actual evapotranspiration E_a, groundwater recharge R and total runoff Q, respectively. The colored lines represent one model each, the gray-black lines represent different observational datasets, labeled on the outer-right panels. The MacDonald groundwater recharge dataset only contains enough data values for the dry-warm region and is thus only shown there. The lines connect binned medians (10 bins along the x-axis with equal amount of points per bin) for each climate region. Note that the axes are capped.

(Figure 3). The relative differences are larger for dry places, commonly perceived as regions where runoff is more difficult to model[55]. Model- and observation-based relationships disagree particularly strongly in dry-cold regions. There, GSIM[56,57] produces little runoff for low precipitation values but then increases faster than any of the models, while GRUN[58] shows almost no increase with increasing precipitation. The Budyko equation and GRUN[58] indicate, in line with an earlier evaluation[59], that most models produce too much total runoff. This parallels recent findings that Earth system models predict higher runoff due to climate change than observations suggest[27]. The overestimation in total runoff is complementary to the underestimation of actual evapotranspiration, and show that most models partition too much precipitation into runoff rather than evapotranspiration.

Diverging dominance of forcing variables on response variables in models

To quantitatively compare the strength of the forcing-response relationships, we use Spearman rank correlations ρ_s. A rank correlation close to 1 (or -1) indicates that the spatial variability in the forcing variable almost completely explains the spatial variability in the response variable, as can be seen in Figure 2a for WaterGAP2. A rank correlation closer to 0 indicates that other factors control the response (e.g. other input or model parameters describing the land surface), as can be seen in Figure 2a for PCR-GLOBWB. We stress that a high correlation is not a measure of goodness of fit. A lot of scatter and correspondingly low correlations might indeed be characteristic for many relationships, and, if underestimated by models, also indicates unrealistic behavior. Calculating rank correlations for all variable pairs, we find that the models differ substantially between each other and in comparison with observations (see Figure 4, Table 1, and Table S3 for all model-based rank correlations).

For precipitation and actual evapotranspiration (Figure 4a), the models show the same ranking between climate regions and rather small differences in magnitude, indicating that actual evapotranspiration is strongly constrained by the available water in all models. The correlations are higher in dry regions (ρ_s=0.74-0.98) than in wet regions (0.57-0.83), reflecting water- and energy-limitations. FLUXCOM tends to show lower correlations, and contrary to the models and the Budyko equation, shows higher values for wet-cold than for dry-cold places. The Budyko equation assumes complete dependence on aridity (here defined as N/P). It thus predicts higher correlations overall and mainly distinguishes between wet (0.83-0.84) and dry (0.98-1.00) regions and, unlike models and FLUXCOM, not between cold and warm regions. The Budyko equation should thus be seen as a useful comparison, but not as the "correct" model, given that different studies have shown that snow[60], climate seasonality[61], vegetation type[62], and inter-catchment groundwater flow[63] can affect the long-term water balance beyond aridity.

We find much variability for net radiation and actual evapotranspiration (Figure 4b). There is no obvious correspondence between the potential evapotranspiration scheme used[49] (e.g. Priestley-Taylor for LPJmL and WaterGAP2, or Penman-Monteith for JULES-W1 and CWatM) and the rank correlations, implying that other factors play a more important role (see also[16,64]). Both the Budyko equation and FLUXCOM show very high correlations for all wet places (0.93-0.99), indicating a strong energy limitation[65], underestimated by many models (especially CWatM and MATSIRO). While FLUXCOM shows a weaker P-E_a-relationship (Figure 4a) in dry-cold places than all models and the Budyko equation, it shows a stronger N-E_a-relationship there (Figure 4b). This could be due to poor representation of energy balance processes in cold regions, possibly related to interactions between snow-affected albedo and evapotranspiration[66,67], sublimation[68], or the aerodynamic component of potential evapotranspiration[69].

For precipitation and groundwater recharge (Figure 4c), some models (CLM4.5, MATSIRO, WaterGAP2 and H08) show high to very high correlations (0.71-0.95) for all climate regions, suggesting that precipitation is the dominant control on groundwater recharge across all climate regions in these models. Other models (CWatM, JULES-W1, LPJmL, PCR-GLOBWB) show much lower and more variable correlations (0.35-0.85), suggesting different controls on groundwater recharge (e.g. model structural decisions and parameterizations). H08 and WaterGAP2 use the same approach to calculate groundwater recharge[49] and they show almost identical rank correlations, indicating that the functional relationships might be relatable to the model structure in this case. Recent studies have shown a strong influence of precipitation and aridity on groundwater recharge[52–54], and using the same datasets, we also find high to very high correlations in dry-warm regions (0.74-0.84). In these often highly water-limited regions, precipitation appears to be the dominant control on groundwater recharge. Besides climate, perceptual models of groundwater recharge generation usually include soil characteristics, topography, land use, and geology[70,71]. This might explain why observations show a more scattered P-R-relationship, particularly in wet-warm regions (-0.05).

For precipitation and total runoff (Figure 4e), WaterGAP2 and PCR-GLOBWB both show lower correlations (0.52-0.75) than most other models (0.77-0.95 for CLM4.5, CWatM, H08, LPJmL, and MATSIRO). This suggests clear differences in how strongly total runoff is controlled by precipitation and in how these models generate runoff. WaterGAP2 is the only model here that is calibrated against streamflow observations[49], which might explain why it shows the lowest rank correlations for total runoff. The Budyko framework assumes that long-term runoff only depends on aridity and thus shows higher correlations (0.87-0.99) than the datasets (0.27-0.89) and most models (0.52-0.95). Given that other factors have been shown to influence total runoff beyond aridity[60–63], and given that GSIM tends to show lower correlations (0.73-0.89), models that show correlations as high as the Budyko equation likely overestimate how strongly precipitation controls total runoff. We generally find the largest differences in both models and datasets in dry-cold regions, where GRUN shows a particularly low correlation (0.27).

For net radiation and both groundwater recharge and total runoff (Figure 4d,f), we find high variability and mostly positive correlations. The models probably produce more groundwater recharge and total runoff in regions with higher net radiation because precipitation is also higher in these regions (see Figure S1 in the Supplementary Information). While it is difficult to interpret these correlations, the large variability still suggests considerable differences between models.

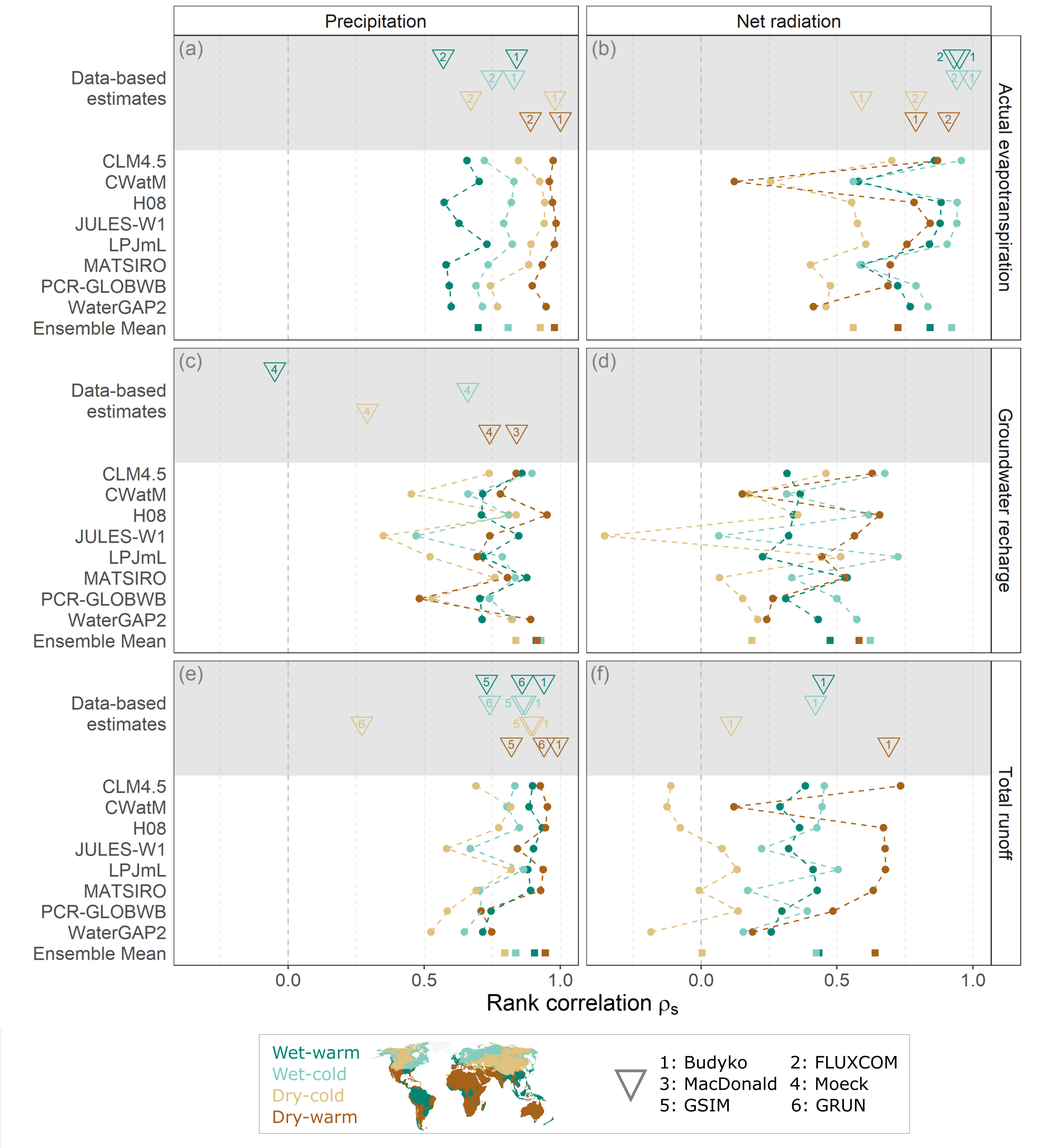

Figure 4. Spearman rank correlations ρ_s between forcing variables (precipitation, net radiation) and water fluxes (actual evapotranspiration, groundwater recharge, and total runoff), divided into different climate regions. Net radiation for LPJmL and PCR-GLOBWB is not available and is estimated as the median of the other models (per grid cell). The lines connecting the dots are only there as a visual aid. The numbered triangles show observation-based rank correlations, with numbers indicating the corresponding data source (see Table 1). Observation-based rank correlations are only shown if they are based on more than 50 data points.

3 Discussion

Focus areas for model improvement

Our analysis has revealed substantial disagreement between models and between models and observations, questioning the robustness of model-based studies and impact assessments, especially if only a single model is used. The energy balance, from total radiation to actual evapotranspiration, appears to be poorly represented, indicated by a different energy limit (Figure 3), a general underestimation of actual evapotranspiration, and widely varying N-E_a-relationships (Figure 4). This warrants a closer look in future studies, as a realistic depiction of energy balance and evaporation processes is critical for climate change studies[65,66]. We find the largest disagreement for groundwater recharge, which is arguably the least understood process and is poorly constrained by observations[52,53,72]. The inter-model differences in groundwater recharge can be much larger than the differences in actual evapotranspiration, and must therefore have other reasons. To better constrain the large variability between models, we need to improve our understanding of the dominant controls on groundwater recharge at large scales[73]. This knowledge is important for assessments of sustainable use of groundwater resources[11,12], for groundwater modeling studies that use groundwater recharge from global water models as input[74,75], and for understanding the sensitivity of groundwater recharge to changing climatic drivers[7]. Most models overestimate total runoff and we find the largest disagreement for total runoff in dry-cold regions. This echoes existing literature[1,14,27,59] and highlights the need for model refinement in dry and/or cold regions, which are under-researched and strongly affected by climate change[55,76]. Given the complementary nature of actual evapotranspiration and total runoff, jointly evaluating their behavior will be valuable for model evaluation and improvement[30,31,33].

Towards an inventory of robust functional relationships

We have collected several observational or observation-based datasets to derive empirical functional relationships, but challenges remain. Observation-based estimates contain uncertainty, inherited from the observational datasets themselves and because not all datasets come with corresponding forcing and response variables (see Methods for an extended discussion). For some variables, small numbers of observations make it difficult to provide robust observation-based constraints for certain regions (see Table 1). For example, groundwater recharge measurements have almost entirely been made in dry-warm regions (97% of[52] and 92% of[53]), leaving groundwater recharge in other regions less well constrained. Most streamflow measurements have been taken in wet regions (60% of GSIM data used here), and globally there is a placement bias of stream gauges towards wet regions[77], even though – according to our classification – short of two-thirds of the global land area are dry. While this spatial bias has clear reasons, from a scientific point of view it should motivate us to rethink where and what to measure. Instead of taking new measurements to understand a specific place, new measurements would have much more leverage if they would help us to also understand other places, e.g. by filling an observational gap along a climatic gradient. In addition, more quality-controlled datasets with uncertainty estimates[52] are critical to obtain realistic uncertainty estimates for functional relationships. This would ultimately allow us to obtain robust ranges of functional behavior which we can benchmark our models against.

While visual comparison (focusing on the shape of the relationships) and rank correlations (focusing on the strength of the relationships) have exposed clear differences between models and observations, our approach here should be seen as a first step. There are other ways to describe the relationships analyzed here, e.g. by characterizing thresholds or non-linearities (visible in Figure 3). Metrics like rank correlations also require careful interpretation. For example, positive correlations between net radiation and groundwater recharge likely arise because precipitation and net radiation are positively correlated, and thus do not imply a causal relationship. The interpretation of empirical relationships should therefore be backed up by process knowledge or extended by methods that allow for discovery of causal relationships[78]. Physics-aware machine learning might be powerful in that respect, as it combines domain knowledge with versatile pattern recognition[79]. Beyond the relationships investigated here, we anticipate that exploring temporal relationships (e.g. by using elasticities[25–27] or shifts in P-Q-relationships[28]), dividing the landscape into different categories (e.g. hydrobelts[80]), and including other variables, such as state variables or stores (e.g. soil moisture, terrestrial water storage), will provide many additional insights.

Conclusions

As our models grow in complexity, encompassing more processes and covering larger spatial and temporal scales, we need a concurrent development of model evaluation: a theory of evaluation for large-scale models. Central to such a theory of evaluation should be hydrological relationships, which shift the focus away from matching historical records in specific locations to a more diagnostic and process-oriented evaluation of model behavior[37]. Functional relationships allow us to focus on larger-scale assessments, to relate places to each other, and to explore if dominant controls in models are consistent with observations, theory and expectations (i.e. our perceptual model[22]). This is critical for ensuring that models faithfully represent real-world systems, leading to more credible projections of environmental change impacts. The large disagreement between models and the lack of observation-based constraints for some variables make a case for the use of a model ensemble to reflect the current uncertain state of knowledge, yet even the ensemble spread might not capture all epistemic uncertainties[81]. Eventually, expanding our range of functional relationships, constrained by various observational datasets and expert knowledge, might give us a knowledge base of realistic system behavior that can be used to evaluate models, diagnose model deficiencies, and weight model ensembles, similar to the use of emergent constraints in climate modeling[38].

More generally, functional relationships invite us to think about how the global water cycle functions, what we know, what we do not know, and what that means for a future under climate change[22]. Our results suggest that improved process understanding will be particularly important for energy balance processes, groundwater recharge processes, and generally in dry and/or cold regions. So how can we improve our process understanding? In 1986, Eagleson[82] stated that "science advances on two legs, analysis and experimentation, and at any moment one is ahead of the other. At the present time advances in hydrology appear to be data limited". For some processes, this still seems to be the case. But clearly, we have a wealth of data available and might ask ourselves: are we extracting enough information from the observations we have? Based on the data we have, what and where should we measure next? And are there hydrological regularities yet to be found[23]? Even if the search for such regularities is challenging, it will be a fruitful and exciting endeavor for global hydrology.

Table 1. Spearman rank correlations ρ_s between forcing variables and water fluxes and number of observations based on different observation-based datasets and the Budyko equation. The percentage of grid cells per climate region is given in brackets. The Budyko equation was forced per grid cell with the same forcing as the models (indicated by *), and thus covers approximately the same extent (except for cells with negative net radiation). The gridded datasets (FLUXCOM, GRUN) are available at the same resolution as the models and thus also cover approximately the same extent (except for non-vegetated areas in the case of FLUXCOM). This is indicated by *m.e.* for model extent. For datasets without matching precipitation data, we used GSWP3 reanalysis data. *Nr* corresponds to the numbers used in Figure 4. The MacDonald rank correlation for the wet-warm region is shown in brackets because of the very small sample size; it is not shown in Figure 4. Dashes (-) indicate that correlations could not be calculated because no observations were available.

Flux	Forcing	Source	Nr	Wet-warm (15%)		Wet-cold (23%)		Dry-cold (28%)		Dry-warm (34%)	
				ρ_s	Count	ρ_s	Count	ρ_s	Count	ρ_s	Count
E_a	P	Budyko*[24]	1	0.84	m.e.	0.83	m.e.	0.98	m.e.	1.00	m.e.
E_a	P	FLUXCOM[50]	2	0.57	m.e.	0.75	m.e.	0.67	m.e.	0.89	m.e.
E_a	N	Budyko*[24]	1	0.95	m.e.	0.99	m.e.	0.59	m.e.	0.79	m.e.
E_a	N	FLUXCOM[50]	2	0.93	m.e.	0.94	m.e.	0.79	m.e.	0.91	m.e.
R	P	MacDonald[52]	3	(0.0)	4	-	0	-	0	0.84	130
R	P	Moeck[53]	4	-0.05	234	0.66	83	0.29	100	0.74	4772
Q	P	Budyko*[24]	1	0.94	m.e.	0.87	m.e.	0.90	m.e.	0.99	m.e.
Q	P	GSIM[56,57]	5	0.73	1438	0.86	1255	0.89	593	0.82	1207
Q	P	GRUN[58]	6	0.86	m.e.	0.74	m.e.	0.27	m.e.	0.94	m.e.
Q	N	Budyko*[24]	1	0.45	m.e.	0.42	m.e.	0.11	m.e.	0.69	m.e.

Methods

Model data retrieval and processing

We analyzed 30-year (climatological) averages (1975-2004) from 8 global water models[48]: CLM4.5[40], CWatM[41], H08[42], JULES-W1[43], LPJmL[44], MATSIRO[45], PCR-GLOBWB[46], and WaterGAP2[47]. The model simulations were carried out following the ISIMIP 2b protocol and here we used model outputs forced with the Earth system model HadGEM2-ES under historical conditions (historical climate and CO_2 concentrations). We note that the specific forcing chosen does not appear to influence model-based functional relationships (see below). We used precipitation P (ISIMIP variable name *pr*), net radiation N (not an official ISIMIP output), actual evapotranspiration E_a (ISIMIP variable name *evap*), groundwater recharge R (ISIMIP variable name *qr*) and total runoff Q (ISIMIP variable name *qtot*). Note that Q here refers to runoff generated on the land fractions (and not surface water bodies) of each grid cell and does not include upstream inflows, which allows for comparison to grid cell P. P, E_a, R, and Q were downloaded from `https://data.isimip.org/`. Net radiation N is not an official ISIMIP output and was provided by the individual modeling groups. It is not available for all models, so we used the ensemble mean per grid cell for models without N data. We converted all fluxes to mm/yr and removed E_a values larger than 10000 mm/yr and set R values smaller than 0 to 0. A more detailed description is given in the Supplementary Information.

CoV and most deviating model maps

For each grid cell, we calculated the coefficient of variation (CoV) by dividing the standard deviation by the mean using the 8 model outputs. Maps of the standard deviation are shown in the Supplementary Information (Figures S8-10). To see which model dominates the ensemble spread, we checked for each grid cell which model shows the largest absolute difference (denoted by d_1) from the ensemble mean (denoted by μ). To see if multiple models dominate the ensemble spread, we also checked for each grid cell which model shows the second largest absolute difference (denoted by d_2) from the ensemble mean. If the relative difference between the largest and the second largest difference is less than 20%, i.e. $(d_1 - d_2)/d_1 < 0.2$, the grid cell falls into the category "multiple". If the relative difference between the most deviating model and the ensemble mean is less than 20%, i.e. $d_1/\mu < 0.2$, the grid cell is counted as having no most deviating model (empty areas on Figure 1d-f).

Functional relationships

To visualize the shape of the functional relationships, we binned the data in each climate region into 10 bins (along the x-axis) with an equal amount of points, calculated the median per bin, and connected the obtained median value. For groundwater recharge, we only used 5 bins because there are so few values. Note that the non-gridded observational datasets do not have the same spatial distribution as the gridded datasets and the models, and thus do not have the same distribution of forcing variables. Their bins can therefore span different ranges of the forcing variables. As a metric for the strength of the functional relationships, we calculate Spearman rank correlations ρ_s between model inputs and outputs per climate region, a measure of the monotonicity between two variables that is robust to outliers. We use the following categories for correlations: negative correlation (<0), no to low correlation (0 to 0.25), medium correlation (0.25-0.5), high correlation (0.5-0.75), very high correlation (0.75-1.0). We also show mean fluxes and slopes obtained through linear regression in the Supplementary Information (Tables S4-S7).

Climate regions

Based on the aridity index (here defined as N/P; where N is model ensemble median), a place is categorized as either wet ($N/P < 1$) or dry ($N/P > 1$). Based on how many days per year fall below a 1°C temperature threshold, a place is categorized as either cold (more than one month below 1°C) or warm (less than one month below 1°C). This results in four categories: wet-warm (15% of model grid cells / 18% of modeled area), wet-cold (23% / 15%), dry-cold (28% / 24%), and dry-warm (34% / 43%). To test how different decisions affect our climate region classification, we also used the ensemble median of potential evapotranspiration E_p (partially downloaded, partially provided by the modeling groups) to calculate the aridity index (E_p/P), and we used a different threshold for our warm/cold distinction. This resulted in little differences overall, as can be seen in the Supplementary Information (Figure S14).

Observational datasets and theory

For E_a, we used FLUXCOM data[50] (RS monthly 0.5° from 2001-2015) paired with GSWP3 P data[83] (downloaded from https://data.isimip.org/). For R, we used data from MacDonald et al.[52] which include matching P data, and data from Moeck et al.[53] paired with GSWP3 P data[83]. For Q, we used GRUN data[58] from 1985-2004 paired with GSWP3 P data[83], and GSIM data[56,57] from catchments with areas from 250-25000 km^2 with minimum 10y of data to ensure a sufficient number of catchments that do not differ too much in size from the model grid cells. We paired GSIM data with catchment-averaged MSWEP P data[84], which were calculated by Stein et al.[85]. To obtain theory-based estimates for E_a and Q, we forced the Budyko[24] equation (Eq.1) with HadGEM2-ES P and ensemble median N from the ISIMIP 2b models analyzed here.

$$\frac{E_a}{P} = \sqrt{\frac{N}{P}\tanh\left(\frac{P}{N}\right)\left(1-\exp\left(-\frac{N}{P}\right)\right)} \tag{1}$$

More details on data processing and quality checks can be found in the Supplementary Information.

Extended discussion on model forcing and scenario uncertainty

The choice of forcing product and differences in the treatment of human influences (e.g. water use and dams) might affect the functional relationships exhibited by the models. To get an idea how much uncertainty this introduces, we calculated correlations using WATCH-WFDEI forcing with either variable historical conditions (varsoc) or no human influences (nosoc) for WaterGAP2 and PCR-GLOBWB, carried out following the ISIMIP 2a protocol. The results, shown in the Supplementary Information, stay essentially the same, showing that the model-based correlations are robust signatures of model behavior.

Extended discussion on data uncertainty

Since not all datasets come with matching P data, we sometimes paired the observations with GSWP3 reanalysis data[83]. To get an idea how much uncertainty this introduces, we investigated how different P data sources affect functional relationships. Correlations calculated using the MacDonald et al.[52] R data with either GSWP3 P data or the accompanying P data are very similar for dry-warm places (0.83 and 0.84; see Supplementary Information). Using HadGEM2-ES P (the model forcing) data instead of GSWP3 P data to calculate correlations with FLUXCOM E_a[50], Moeck R[53], and GRUN Q[58], respectively, results in virtually no differences (results are shown in the Supplementary Information). Since most datasets only contain a limited number of years of data, sometimes only one average value[52,53], we used all available years in our analysis. The only observation-based dataset that contains long enough time series to analyze functional relationships for two independent 30-year periods is GRUN[58]. Using GRUN data from 1945-1974 instead of 1975-2004 results in virtually no differences (see Supplementary Information). While we cannot rule out that other datasets would lead to different relationships, this analysis indicates that the functional relationships and the rank correlations are relatively robust.

Data availability

The long-term averages created and used in this study are deposited at https://zenodo.org/record/7714885. Correlations and other statistics are available in the Supporting Information. Data used in this study can be downloaded from the following links. ISIMIP 2b data (model outputs and GSWP3 precipitation data) are available from https://www.isimip.org/. FLUXCOM data are available from http://www.fluxcom.org/. MacDonald et al. recharge data are available from https://www2.bgs.ac.uk/nationalgeosciencedatacentre/citedData/catalogue/45d2b71c-d413-44d4-8b4b-6190527912ff.html. Contains data supplied by permission of the Natural Environment Research Council [2022]. Moeck et al. recharge data are available from https://opendata.eawag.ch/dataset/globalscale_groundwater_moeck. GSIM data are available from https://doi.pangaea.de/10.1594/PANGAEA.887477 and https://doi.pangaea.de/10.1594/PANGAEA.887470. MSWEP data can be requested for research purposes from http://www.gloh2o.org/mswep/.

Code availability

Python and R codes used to perform the analysis are available at `https://github.com/HydroSysPotsdam/GHM_Comparison`.

Acknowledgements

SJG, RR, LS, and TW acknowledge support from the Alexander von Humboldt Foundation in the framework of the Alexander von Humboldt Professorship endowed by the German Federal Ministry of Education and Research (BMBF). This publication is based upon work from COST Action CA19139 – PROCLIAS, supported by COST (European Cooperation in Science and Technology, `https://www.cost.eu`). We thank Petra Döll for providing helpful comments on the manuscript. We also thank the ISIMIP team for their continued efforts within the ISIMIP project.

Author contributions

SJG, RR, LS, and TW designed the study. YW, WT, HMS, YS, YP, SO, AK, NH, MG, and PB conducted hydrological simulations under the ISIMIP2b project and SNG and HMS coordinated the ISIMIP global water sector. SJG and RR processed the simulation results, conducted the analyses, and SJG, RR, and LS prepared the graphics. SJG wrote the first paper draft together with RR, LS, and TW. All authors contributed to discussion and interpretations of the results and writing the paper.

References

1. Gädeke, A. *et al.* Performance evaluation of global hydrological models in six large Pan-Arctic watersheds. *Clim. Chang.* **163**, 1329–1351, DOI: 10.1007/s10584-020-02892-2 (2020).

2. IPCC. *Climate Change 2022: Impacts, Adaptation, and Vulnerability. Contribution of Working Group II to the Sixth Assessment Report of the Intergovernmental Panel on Climate Change [H.-O. Pörtner, D.C. Roberts, M. Tignor, E.S. Poloczanska, K. Mintenbeck, A. Alegría, M. Craig, S. Langsdorf, S. Löschke, V. Möller, A. Okem, B. Rama (eds.)]* (Cambridge University Press, 2022).

3. Samaniego, L. *et al.* Anthropogenic warming exacerbates European soil moisture droughts. *Nat. Clim. Chang.* **8**, 421–426, DOI: 10.1038/s41558-018-0138-5 (2018). Number: 5 Publisher: Nature Publishing Group.

4. Schewe, J. *et al.* Multimodel assessment of water scarcity under climate change. *Proc. Natl. Acad. Sci.* **111**, 3245–3250, DOI: 10.1073/pnas.1222460110 (2014). Publisher: Proceedings of the National Academy of Sciences.

5. Gudmundsson, L. *et al.* Globally observed trends in mean and extreme river flow attributed to climate change. *Science* **371**, 1159–1162, DOI: 10.1126/science.aba3996 (2021). Publisher: American Association for the Advancement of Science.

6. Pokhrel, Y. *et al.* Global terrestrial water storage and drought severity under climate change. *Nat. Clim. Chang.* **11**, 226–233, DOI: 10.1038/s41558-020-00972-w (2021). Number: 3 Publisher: Nature Publishing Group.

7. Reinecke, R. *et al.* Uncertainty of simulated groundwater recharge at different global warming levels: a global-scale multi-model ensemble study. *Hydrol. Earth Syst. Sci.* **25**, 787–810, DOI: 10.5194/hess-25-787-2021 (2021). Publisher: Copernicus GmbH.

8. IGRAC. Global Groundwater Information System (2022). Published: ggis.un-igrac.org.

9. Sheffield, J. *et al.* A Drought Monitoring and Forecasting System for Sub-Sahara African Water Resources and Food Security. *Bull. Am. Meteorol. Soc.* **95**, 861–882, DOI: 10.1175/BAMS-D-12-00124.1 (2014). Publisher: American Meteorological Society Section: Bulletin of the American Meteorological Society.

10. Döll, P. & Fiedler, K. Global-scale modeling of groundwater recharge. *Hydrol. Earth Syst. Sci.* **12**, 863–885, DOI: 10.5194/hess-12-863-2008 (2008). Publisher: Copernicus GmbH.

11. Wada, Y. *et al.* Global depletion of groundwater resources. *Geophys. Res. Lett.* **37**, DOI: 10.1029/2010GL044571 (2010). _eprint: https://onlinelibrary.wiley.com/doi/pdf/10.1029/2010GL044571.

12. Richey, A. S. *et al.* Quantifying renewable groundwater stress with GRACE. *Water Resour. Res.* **51**, 5217–5238, DOI: 10.1002/2015WR017349 (2015). _eprint: https://onlinelibrary.wiley.com/doi/pdf/10.1002/2015WR017349.

13. Prudhomme, C. *et al.* Hydrological droughts in the 21st century, hotspots and uncertainties from a global multimodel ensemble experiment. *Proc. Natl. Acad. Sci.* **111**, 3262–3267, DOI: 10.1073/pnas.1222473110 (2014). Publisher: Proceedings of the National Academy of Sciences.

14. Giuntoli, I., Vidal, J.-P., Prudhomme, C. & Hannah, D. M. Future hydrological extremes: the uncertainty from multiple global climate and global hydrological models. *Earth Syst. Dyn.* **6**, 267–285, DOI: 10.5194/esd-6-267-2015 (2015). Publisher: Copernicus GmbH.

15. Beck, H. E. *et al.* Global evaluation of runoff from 10 state-of-the-art hydrological models. *Hydrol. Earth Syst. Sci.* **21**, 2881–2903, DOI: 10.5194/hess-21-2881-2017 (2017). Publisher: Copernicus GmbH.

16. Wartenburger, R. *et al.* Evapotranspiration simulations in ISIMIP2a—Evaluation of spatio-temporal characteristics with a comprehensive ensemble of independent datasets. *Environ. Res. Lett.* **13**, 075001, DOI: 10.1088/1748-9326/aac4bb (2018). Publisher: IOP Publishing.

17. Gleeson, T. *et al.* GMD perspective: The quest to improve the evaluation of groundwater representation in continental- to global-scale models. *Geosci. Model. Dev.* **14**, 7545–7571, DOI: 10.5194/gmd-14-7545-2021 (2021). Publisher: Copernicus GmbH.

18. Hrachowitz, M. *et al.* A decade of Predictions in Ungauged Basins (PUB)—a review. *Hydrol. Sci. J.* **58**, 1198–1255, DOI: 10.1080/02626667.2013.803183 (2013). Publisher: Taylor & Francis _eprint: https://doi.org/10.1080/02626667.2013.803183.

19. Peel, M. C. & Blöschl, G. Hydrological modelling in a changing world. *Prog. Phys. Geogr. Earth Environ.* **35**, 249–261, DOI: 10.1177/0309133311402550 (2011).

20. Wagener, T., Reinecke, R. & Pianosi, F. On the evaluation of climate change impact models. *WIREs Clim. Chang.* **13**, e772, DOI: 10.1002/wcc.772 (2022). _eprint: https://onlinelibrary.wiley.com/doi/pdf/10.1002/wcc.772.

21. O, S., Dutra, E. & Orth, R. Robustness of Process-Based versus Data-Driven Modeling in Changing Climatic Conditions. *J. Hydrometeorol.* **21**, 1929–1944, DOI: 10.1175/JHM-D-20-0072.1 (2020). Publisher: American Meteorological Society Section: Journal of Hydrometeorology.

22. Wagener, T. *et al.* On doing hydrology with dragons: Realizing the value of perceptual models and knowledge accumulation. *WIREs Water* **8**, e1550, DOI: 10.1002/wat2.1550 (2021). _eprint: https://onlinelibrary.wiley.com/doi/pdf/10.1002/wat2.1550.

23. Dooge, J. C. I. Looking for hydrologic laws. *Water Resour. Res.* **22**, 46S–58S, DOI: 10.1029/WR022i09Sp0046S (1986). _eprint: https://onlinelibrary.wiley.com/doi/pdf/10.1029/WR022i09Sp0046S.

24. Budyko, M. I. Climate and life. Tech. Rep. 18, Academic Press (1974). ISBN: 9780121394509.

25. NĚMEC, J. & SCHAAKE, J. Sensitivity of water resource systems to climate variation. *Hydrol. Sci. J.* **27**, 327–343, DOI: 10.1080/02626668209491113 (1982). Publisher: Taylor & Francis _eprint: https://doi.org/10.1080/02626668209491113.

26. Sankarasubramanian, A., Vogel, R. M. & Limbrunner, J. F. Climate elasticity of streamflow in the United States. *Water Resour. Res.* **37**, 1771–1781, DOI: 10.1029/2000WR900330 (2001). _eprint: https://onlinelibrary.wiley.com/doi/pdf/10.1029/2000WR900330.

27. Zhang, Y. *et al.* Future global streamflow declines are probably more severe than previously estimated. *Nat. Water* 1–11, DOI: 10.1038/s44221-023-00030-7 (2023). Publisher: Nature Publishing Group.

28. Peterson, T. J., Saft, M., Peel, M. C. & John, A. Watersheds may not recover from drought. *Science* **372**, 745–749, DOI: 10.1126/science.abd5085 (2021). Publisher: American Association for the Advancement of Science.

29. Koster, R. D. & Milly, P. The Interplay between Transpiration and Runoff Formulations in Land Surface Schemes Used with Atmospheric Models. *J. Clim.* **10** (1997).

30. Dirmeyer, P. A., Koster, R. D. & Guo, Z. Do Global Models Properly Represent the Feedback between Land and Atmosphere? *J. Hydrometeorol.* **7**, 1177–1198, DOI: 10.1175/JHM532.1 (2006). Publisher: American Meteorological Society Section: Journal of Hydrometeorology.

31. Koster, R. "Efficiency Space": A Framework for Evaluating Joint Evaporation and Runoff Behavior. *Bull. Am. Meteorol. Soc.* **96**, 393–396, DOI: 10.1175/BAMS-D-14-00056.1 (2015). Publisher: American Meteorological Society Section: Bulletin of the American Meteorological Society.

32. L'vovich, M. I. *World water resources and their future* (AGU, Washington, DC (USA), 1979).

33. Koster, R. D. & Mahanama, S. P. P. Land Surface Controls on Hydroclimatic Means and Variability. *J. Hydrometeorol.* **13**, 1604–1620, DOI: 10.1175/JHM-D-12-050.1 (2012). Publisher: American Meteorological Society Section: Journal of Hydrometeorology.

34. Kapangaziwiri, E., Hughes, D. & Wagener, T. Incorporating uncertainty in hydrological predictions for gauged and ungauged basins in southern Africa. *Hydrol. Sci. J.* **57**, 1000–1019, DOI: 10.1080/02626667.2012.690881 (2012). Publisher: Taylor & Francis _eprint: https://doi.org/10.1080/02626667.2012.690881.

35. Troy, T. J., Wood, E. F. & Sheffield, J. An efficient calibration method for continental-scale land surface modeling. *Water Resour. Res.* **44**, DOI: 10.1029/2007WR006513 (2008). _eprint: https://onlinelibrary.wiley.com/doi/pdf/10.1029/2007WR006513.

36. Greve, P., Burek, P. & Wada, Y. Using the Budyko Framework for Calibrating a Global Hydrological Model. *Water Resour. Res.* **56**, e2019WR026280, DOI: 10.1029/2019WR026280 (2020). _eprint: https://onlinelibrary.wiley.com/doi/pdf/10.1029/2019WR026280.

37. Gupta, H. V., Wagener, T. & Liu, Y. Reconciling theory with observations: elements of a diagnostic approach to model evaluation. *Hydrol. Process.* **22**, 3802–3813, DOI: 10.1002/hyp.6989 (2008). _eprint: https://onlinelibrary.wiley.com/doi/pdf/10.1002/hyp.6989.

38. Eyring, V. *et al.* Taking climate model evaluation to the next level. *Nat. Clim. Chang.* **9**, 102–110, DOI: 10.1038/s41558-018-0355-y (2019). Number: 2 Publisher: Nature Publishing Group.

39. Betts, A. K. Understanding Hydrometeorology Using Global Models. *Bull. Am. Meteorol. Soc.* **85**, 1673–1688, DOI: 10.1175/BAMS-85-11-1673 (2004). Publisher: American Meteorological Society Section: Bulletin of the American Meteorological Society.

40. Thiery, W. *et al.* Present-day irrigation mitigates heat extremes. *J. Geophys. Res. Atmospheres* **122**, 1403–1422, DOI: 10.1002/2016JD025740 (2017). _eprint: https://onlinelibrary.wiley.com/doi/pdf/10.1002/2016JD025740.

41. Burek, P. *et al.* Development of the Community Water Model (CWatM v1.04) – a high-resolution hydrological model for global and regional assessment of integrated water resources management. *Geosci. Model. Dev.* **13**, 3267–3298, DOI: 10.5194/gmd-13-3267-2020 (2020). Publisher: Copernicus GmbH.

42. Hanasaki, N., Yoshikawa, S., Pokhrel, Y. & Kanae, S. A global hydrological simulation to specify the sources of water used by humans. *Hydrol. Earth Syst. Sci.* **22**, 789–817, DOI: 10.5194/hess-22-789-2018 (2018). Publisher: Copernicus GmbH.

43. Best, M. J. *et al.* The Joint UK Land Environment Simulator (JULES), model description – Part 1: Energy and water fluxes. *Geosci. Model. Dev.* **4**, 677–699, DOI: 10.5194/gmd-4-677-2011 (2011). Publisher: Copernicus GmbH.

44. Jägermeyr, J. *et al.* Water savings potentials of irrigation systems: global simulation of processes and linkages. *Hydrol. Earth Syst. Sci.* **19**, 3073–3091, DOI: 10.5194/hess-19-3073-2015 (2015). Publisher: Copernicus GmbH.

45. Takata, K., Emori, S. & Watanabe, T. Development of the minimal advanced treatments of surface interaction and runoff. *Glob. Planet. Chang.* **38**, 209–222, DOI: 10.1016/S0921-8181(03)00030-4 (2003).

46. Sutanudjaja, E. H. *et al.* PCR-GLOBWB 2: a 5 arcmin global hydrological and water resources model. *Geosci. Model. Dev.* **11**, 2429–2453, DOI: 10.5194/gmd-11-2429-2018 (2018). Publisher: Copernicus GmbH.

47. Müller Schmied, H. *et al.* Variations of global and continental water balance components as impacted by climate forcing uncertainty and human water use. *Hydrol. Earth Syst. Sci.* **20**, 2877–2898, DOI: 10.5194/hess-20-2877-2016 (2016). Publisher: Copernicus GmbH.

48. Frieler, K. *et al.* Assessing the impacts of 1.5 °C global warming – simulation protocol of the Inter-Sectoral Impact Model Intercomparison Project (ISIMIP2b). *Geosci. Model. Dev.* **10**, 4321–4345, DOI: 10.5194/gmd-10-4321-2017 (2017). Publisher: Copernicus GmbH.

49. Telteu, C.-E. *et al.* Understanding each other's models: an introduction and a standard representation of 16 global water models to support intercomparison, improvement, and communication. *Geosci. Model. Dev.* **14**, 3843–3878, DOI: 10.5194/gmd-14-3843-2021 (2021). Publisher: Copernicus GmbH.

50. Jung, M. *et al.* The FLUXCOM ensemble of global land-atmosphere energy fluxes. *Sci. Data* **6**, 74, DOI: 10.1038/s41597-019-0076-8 (2019). Number: 1 Publisher: Nature Publishing Group.

51. Elnashar, A., Wang, L., Wu, B., Zhu, W. & Zeng, H. Synthesis of global actual evapotranspiration from 1982 to 2019. *Earth Syst. Sci. Data* **13**, 447–480, DOI: 10.5194/essd-13-447-2021 (2021). Publisher: Copernicus GmbH.

52. MacDonald, A. M. *et al.* Mapping groundwater recharge in Africa from ground observations and implications for water security. *Environ. Res. Lett.* **16**, 034012, DOI: 10.1088/1748-9326/abd661 (2021). Publisher: IOP Publishing.

53. Moeck, C. *et al.* A global-scale dataset of direct natural groundwater recharge rates: A review of variables, processes and relationships. *Sci. The Total. Environ.* **717**, 137042, DOI: 10.1016/j.scitotenv.2020.137042 (2020).

54. Berghuijs, W. R., Luijendijk, E., Moeck, C., van der Velde, Y. & Allen, S. T. Global Recharge Data Set Indicates Strengthened Groundwater Connection to Surface Fluxes. *Geophys. Res. Lett.* **49**, e2022GL099010, DOI: 10.1029/2022GL099010 (2022). _eprint: https://onlinelibrary.wiley.com/doi/pdf/10.1029/2022GL099010.

55. Zoccatelli, D. *et al.* Contrasting rainfall-runoff characteristics of floods in desert and Mediterranean basins. *Hydrol. Earth Syst. Sci.* **23**, 2665–2678, DOI: 10.5194/hess-23-2665-2019 (2019). Publisher: Copernicus GmbH.

56. Do, H. X., Gudmundsson, L., Leonard, M. & Westra, S. The Global Streamflow Indices and Metadata Archive (GSIM) – Part 1: The production of a daily streamflow archive and metadata. *Earth Syst. Sci. Data* **10**, 765–785, DOI: 10.5194/essd-10-765-2018 (2018). Publisher: Copernicus GmbH.

57. Gudmundsson, L., Do, H. X., Leonard, M. & Westra, S. The Global Streamflow Indices and Metadata Archive (GSIM) – Part 2: Quality control, time-series indices and homogeneity assessment. *Earth Syst. Sci. Data* **10**, 787–804, DOI: 10.5194/essd-10-787-2018 (2018). Publisher: Copernicus GmbH.

58. Ghiggi, G., Humphrey, V., Seneviratne, S. I. & Gudmundsson, L. GRUN: an observation-based global gridded runoff dataset from 1902 to 2014. *Earth Syst. Sci. Data* **11**, 1655–1674, DOI: 10.5194/essd-11-1655-2019 (2019). Publisher: Copernicus GmbH.

59. Zaherpour, J. *et al.* Worldwide evaluation of mean and extreme runoff from six global-scale hydrological models that account for human impacts. *Environ. Res. Lett.* **13**, 065015, DOI: 10.1088/1748-9326/aac547 (2018). Publisher: IOP Publishing.

60. Berghuijs, W. R., Woods, R. A. & Hrachowitz, M. A precipitation shift from snow towards rain leads to a decrease in streamflow. *Nat. Clim. Chang.* **4**, 583–586, DOI: 10.1038/nclimate2246 (2014). Number: 7 Publisher: Nature Publishing Group.

61. Milly, P. C. D. Climate, soil water storage, and the average annual water balance. *Water Resour. Res.* **30**, 2143–2156, DOI: 10.1029/94WR00586 (1994). _eprint: https://onlinelibrary.wiley.com/doi/pdf/10.1029/94WR00586.

62. Zhang, L., Dawes, W. R. & Walker, G. R. Response of mean annual evapotranspiration to vegetation changes at catchment scale. *Water Resour. Res.* **37**, 701–708, DOI: 10.1029/2000WR900325 (2001). _eprint: https://onlinelibrary.wiley.com/doi/pdf/10.1029/2000WR900325.

63. Liu, Y., Wagener, T., Beck, H. E. & Hartmann, A. What is the hydrologically effective area of a catchment? *Environ. Res. Lett.* **15**, 104024, DOI: 10.1088/1748-9326/aba7e5 (2020). Publisher: IOP Publishing.

64. Haddeland, I. *et al.* Multimodel Estimate of the Global Terrestrial Water Balance: Setup and First Results. *J. Hydrometeorol.* **12**, 869–884, DOI: 10.1175/2011JHM1324.1 (2011). Publisher: American Meteorological Society Section: Journal of Hydrometeorology.

65. Milly, P. C. D. & Dunne, K. A. Potential evapotranspiration and continental drying. *Nat. Clim. Chang.* **6**, 946–949, DOI: 10.1038/nclimate3046 (2016). Number: 10 Publisher: Nature Publishing Group.

66. Milly, P. C. D. & Dunne, K. A. Colorado River flow dwindles as warming-driven loss of reflective snow energizes evaporation. *Science* **367**, 1252–1255, DOI: 10.1126/science.aay9187 (2020). Publisher: American Association for the Advancement of Science.

67. Meira Neto, A. A., Niu, G.-Y., Roy, T., Tyler, S. & Troch, P. A. Interactions between snow cover and evaporation lead to higher sensitivity of streamflow to temperature. *Commun. Earth & Environ.* **1**, 1–7, DOI: 10.1038/s43247-020-00056-9 (2020). Number: 1 Publisher: Nature Publishing Group.

68. Bowling, L. C., Pomeroy, J. W. & Lettenmaier, D. P. Parameterization of Blowing-Snow Sublimation in a Macroscale Hydrology Model. *J. Hydrometeorol.* **5**, 745–762, DOI: 10.1175/1525-7541(2004)005<0745:POBSIA>2.0.CO;2 (2004). Publisher: American Meteorological Society Section: Journal of Hydrometeorology.

69. Tabari, H. & Talaee, P. H. Local Calibration of the Hargreaves and Priestley-Taylor Equations for Estimating Reference Evapotranspiration in Arid and Cold Climates of Iran Based on the Penman-Monteith Model. *J. Hydrol. Eng.* **16**, 837–845, DOI: 10.1061/(ASCE)HE.1943-5584.0000366 (2011). Publisher: American Society of Civil Engineers.

70. Scanlon, B. R., Healy, R. W. & Cook, P. G. Choosing appropriate techniques for quantifying groundwater recharge. *Hydrogeol. J.* 22 (2002).

71. Cuthbert, M. O. *et al.* Observed controls on resilience of groundwater to climate variability in sub-Saharan Africa. *Nature* **572**, 230–234, DOI: 10.1038/s41586-019-1441-7 (2019). Number: 7768 Publisher: Nature Publishing Group.

72. Green, T. R. *et al.* Beneath the surface of global change: Impacts of climate change on groundwater. *J. Hydrol.* **405**, 532–560, DOI: 10.1016/j.jhydrol.2011.05.002 (2011).

73. West, C. *et al.* Ground truthing global-scale model estimates of groundwater recharge across Africa. *Sci. The Total. Environ.* **858**, 159765, DOI: 10.1016/j.scitotenv.2022.159765 (2023).

74. de Graaf, I. E. M. *et al.* A global-scale two-layer transient groundwater model: Development and application to groundwater depletion. *Adv. Water Resour.* **102**, 53–67, DOI: 10.1016/j.advwatres.2017.01.011 (2017).

75. Reinecke, R. *et al.* Challenges in developing a global gradient-based groundwater model (G^3M v1.0) for the integration into a global hydrological model. *Geosci. Model. Dev.* **12**, 2401–2418, DOI: 10.5194/gmd-12-2401-2019 (2019). Publisher: Copernicus GmbH.

76. Felfelani, F., Wada, Y., Longuevergne, L. & Pokhrel, Y. N. Natural and human-induced terrestrial water storage change: A global analysis using hydrological models and GRACE. *J. Hydrol.* **553**, 105–118, DOI: 10.1016/j.jhydrol.2017.07.048 (2017).

77. Krabbenhoft, C. A. *et al.* Assessing placement bias of the global river gauge network. *Nat. Sustain.* 1–7, DOI: 10.1038/s41893-022-00873-0 (2022). Publisher: Nature Publishing Group.

78. Massmann, A., Gentine, P. & Runge, J. Causal inference for process understanding in Earth sciences (2021). ArXiv:2105.00912 [physics].

79. Reichstein, M. *et al.* Deep learning and process understanding for data-driven Earth system science. *Nature* **566**, 195–204, DOI: 10.1038/s41586-019-0912-1 (2019). Number: 7743 Publisher: Nature Publishing Group.

80. Meybeck, M., Kummu, M. & Dürr, H. H. Global hydrobelts and hydroregions: improved reporting scale for water-related issues? *Hydrol. Earth Syst. Sci.* **17**, 1093–1111, DOI: 10.5194/hess-17-1093-2013 (2013). Publisher: Copernicus GmbH.

81. Beven, K. J. *et al.* Epistemic uncertainties and natural hazard risk assessment – Part 2: What should constitute good practice? *Nat. Hazards Earth Syst. Sci.* **18**, 2769–2783, DOI: 10.5194/nhess-18-2769-2018 (2018). Publisher: Copernicus GmbH.

82. Eagleson, P. S. The emergence of global-scale hydrology. *Water Resour. Res.* **22**, 6S–14S, DOI: 10.1029/WR022i09Sp0006S (1986). _eprint: https://onlinelibrary.wiley.com/doi/pdf/10.1029/WR022i09Sp0006S.

83. Dirmeyer, P. A. *et al.* GSWP-2: Multimodel Analysis and Implications for Our Perception of the Land Surface. *Bull. Am. Meteorol. Soc.* **87**, 1381–1398, DOI: 10.1175/BAMS-87-10-1381 (2006). Publisher: American Meteorological Society Section: Bulletin of the American Meteorological Society.

84. Beck, H. E. *et al.* MSWEP V2 Global 3-Hourly 0.1° Precipitation: Methodology and Quantitative Assessment. *Bull. Am. Meteorol. Soc.* **100**, 473–500, DOI: 10.1175/BAMS-D-17-0138.1 (2019). Publisher: American Meteorological Society Section: Bulletin of the American Meteorological Society.

85. Stein, L., Pianosi, F. & Woods, R. Event-based classification for global study of river flood generating processes. *Hydrol. Process.* **34**, 1514–1529, DOI: 10.1002/hyp.13678 (2020). _eprint: https://onlinelibrary.wiley.com/doi/pdf/10.1002/hyp.13678.